



ELEDIA Research Center

*ELEDIA@UniTN - University of Trento
Consorzio Nazionale Interuniversitario*

per le Telecomunicazioni

Via Mesiano 77, I-38123 Trento, Italy

E-mail: contact@eledia.org

Web: www.eledia.org/eledia-unitn



Project **MOSAIC**

Modular Scanning Array based on Simple Antenna Manufacturing

Executive Summary



Author: ELEDIA-CNIT

Version: 1.0

Status: FINAL

Last Revision: 9 December 2024 17:00

Document Index

| | |
|--|----|
| 1. Scope of the Document | 4 |
| 2. Deliverable Reports..... | 5 |
| 3. Summary of the Work..... | 6 |
| 3.1. Background and Introduction | 6 |
| 3.2. Technical Specifications | 7 |
| 3.3. Subarrayed Architecture Optimization Results..... | 8 |
| 3.4. Passive Beam Forming Network Design, Prototype Implementation, and Measurements | 12 |
| 4. Conclusions | 15 |
| 5. References | 15 |

Abbreviations

| | |
|---------|--|
| AESA: | Active Electronically Scanned Array |
| AFR: | Array-Fed Reflector |
| BFN: | Beam Forming Network |
| CP: | Convex Programming |
| D: | Directivity |
| DRA: | Direct Radiating Array |
| GEO: | Geostationary Earth Orbit |
| H-LPF: | Horizontally Printable Low Pass Filter |
| LFoV: | Limited Field of View |
| MOSAIC: | Modular Scanning Array based on Simple Antenna Manufacturing |
| PBFN: | Passive Beam Forming Network |
| RX: | Receive |
| SHE: | Square Horn Element |
| SL: | Scan Loss |
| SLL: | Side Lobe Level |
| SOMT: | Septum Orthomode Transducer |
| TX: | Transmit |
| V-LPF: | Vertically Printable Low Pass Filter |
| XPD: | Cross-Polarization Discrimination |

1. SCOPE OF THE DOCUMENT

This document provides a concise summary of the work performed throughout the MOSAIC project, including an outline of the background information, a brief description of the specification, and the project outcomes.

2. DELIVERABLE REPORTS

| No. | Delivery Date | Title | Deliverable | WP |
|--------|---------------|--|-------------|----|
| D1.1 | 07-07-23 | Finalized Technical Specification | D1.1 | 1 |
| D1.2.1 | 07-07-23 | SoA Survey: Sub-array Optimization Techniques for Array Design | D1.2 | 1 |
| D1.2.2 | 07-07-23 | SoA Survey: All-Metallic Radiating Elements | D1.2 | 1 |
| D1.2.3 | 07-07-23 | SoA Survey: Waveguide Components for Array Tiles | D1.2 | 1 |
| D1.3 | 07-07-23 | Preliminary Verification Plan | D1.3 | 1 |
| D1.4 | 07-07-23 | Selected Antenna Baseline Configuration | D1.4 | 2 |
| D1.5 | 07-07-23 | Preliminary Baseline Design | D1.5 | 2 |
| D1.5.1 | 31-07-23 | Detailed analysis of the solution presented in Deliverable 1.4 based on equal L-shaped tetrominoes | D1.5 | 2 |
| D1.6 | 07-07-23 | Definition of Partial Prototype | D1.6 | 2 |
| D1.7 | 29-11-23 | Detailed Design of the Partial Prototype | D1.7 | 3 |
| D1.8 | 29-11-23 | Confirmation of Feasibility | D1.8 | 3 |
| D1.9 | 01-12-23 | Implementation and Verification Plan | D1.9 | 4 |
| D1.10 | 05-12-24 | Verified Deliverables Items and Compliance Statement | D1.10 | 5 |
| D1.11 | 24-06-24 | Prototype | D1.11 | 5 |
| D1.12 | 05-12-24 | Radiation Pattern Test Report | D1.12 | 5 |
| D1.13 | 05-12-24 | Analysed Test Results & Prediction Consistency Assessment | D1.13 | 5 |
| D1.14 | 05-12-24 | Updated Statement of Compliance | D1.14 | 5 |
| D1.15 | 05-12-24 | Technology Assessment and Development Plan | D1.15 | 6 |

3. SUMMARY OF THE WORK

3.1. BACKGROUND AND INTRODUCTION

The main goal of MOSAIC project consists in the design of an AESA improving the technical and commercial maturity of the antenna architectures proposed in the ESA invention [1] which describes a design and manufacturing method for large sparse phased arrays for geostationary Earth orbit (GEO) satellite. Sparse arrays offer power consumption reduction through a not regular lattice, at the cost of increasing the complexity of the beam forming network (BFN) as well as a not complete filling of the available aperture.

The main idea of MOSAIC consists in adopting:

- a modular structure, based on irregular subarraying [2][3], to simplify the antenna architecture and the BFN as well as to ensure the complete overlay with the tiles modules of the array aperture;
- a passive beam forming network composed by monolithic components to significantly enhance the simplicity and manufacturability of the entire system and compliant with additive manufacturing [4].

3.2. TECHNICAL SPECIFICATIONS

The list of technical specifications for the MOSAIC project has been reported in **Deliverable Report D1.1**. The partner SWISSTO12 proposes as the main goal of the project the reduction of the number of controls in the arrays of payloads for HummingSat mission, and is summarized in Tab. 3.2.1.

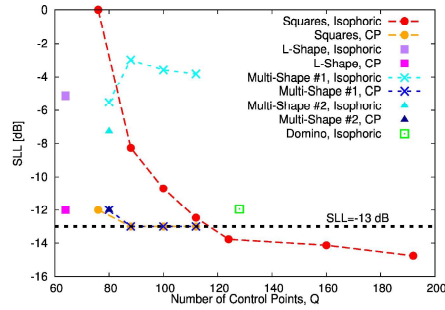
| Specification | Value | Comment |
|---------------------------------------|--|-----------------------|
| Type of antenna | Payload with 1 DRA performing both TX and RX | |
| Frequency | TX: 17.7-20.2 [GHz] RX: 27.5-30 [GHz] | |
| Field of view | +/- 8 [deg] | without grating lobes |
| Number of Radiating Elements | DRA with 16x16 radiating elements | |
| Radiating Elements Spacing | Square lattice with 3.5 [λ] | λ @ 30 GHz |
| Directivity (D) | To be maximized, considering the number of ports | |
| Scan Loss (SL) | To be minimized | |
| Side Lobe Level (SLL) | ≤ -13 [dB] | |
| Polarization | Single circular polarization | TX: RHCP RX: LHCP |
| Radiating Element Aperture efficiency | > 80% | |
| XPD | > 21 dB | in field of view |
| Radiating Element Topology | - Dual-band square horn - Dual-band Septum polarizer - Diplexer with input and output filter | |

Table 3.2.1. Technical specifications for payload with 1 DRA performing both TX and RX.

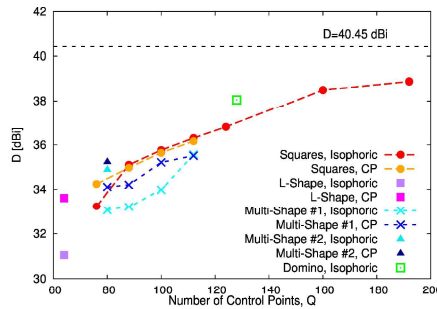
3.3. SUBARRAYED ARCHITECTURE OPTIMIZATION RESULTS

The sub-array configurations have been optimized considering the following sets of tiles shapes.

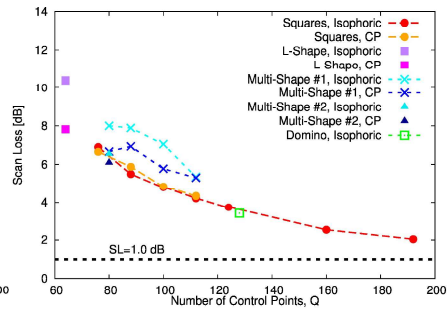
| | |
|---|---|
| <p>Single Domino Shape</p> | |
| <p>Squares Shapes</p> | <p>Square 1 x 1 (i.e., Single Element)</p> <p>Square 2 x 2</p> <p>Square 4 x 4</p> |
| <p>Single L-Shape (L-Tetromino)</p> | <p>L Tetromino</p> |
| <p>Multi-Shapes #1 (Squares + L-Tetromino)</p> | <p>Square 1 x 1 (i.e., Single Element)</p> <p>Square 2 x 2</p> <p>Square 3 x 3</p> <p>L Tetromino</p> |
| <p>Multi-Shapes #2 (L-Tromino + L-Tetromino)</p> | <p>L Tromino</p> <p>L Tetromino</p> |



(a)



(b)



(c)

Figure 3.3.1 Pareto optimal solutions trade-off between the number of control points, Q , and the (a) SLL, (b) directivity, and (c) scan loss.

All the optimization details are reported in **Deliverable Report D1.4** and summarized in Fig. 3.3.1 showing the Pareto front of the executed optimizations considering several trade-off between the number of control points, Q , and the SLL, Directivity, and Scan-Loss. The corresponding numerical value are summarized in Tab. 3.3.2 when considering isophoric amplification coefficients such to enable the operation of amplifiers all in saturation mode. Moreover, the tiles amplitude and phase coefficients have been optimized using a Convex Programming (CP) method in order to show the possibility to control the SLL by reconfiguring the amplitude/phase weights (Tab. 3.3.3). From the Pareto front of the executed optimizations two solutions have been selected for the technical baseline preliminary design, and analyzed in detail (in both the TX and RX band) in **Deliverable Report D1.5**:

- **Solution #1**: the Squares-Shapes solution [Fig. 3.3.2(a)] with **$Q = 112$ control points** (i.e., a 56% reduction with respect to the fully-populated array);
- **Solution #2**: the Multi-Shape #2 solution [Fig. 3.3.2(b)] with **$Q = 80$ control points** (i.e., a 69% reduction with respect to the fully-populated array);

| Architecture | Number of Control Points | Control Points Reduction | Scan Angle (θ, ϕ) [deg] | SLL [dB] | Directivity [dBi] | Scan-Loss [dB] |
|----------------------|--------------------------|--------------------------|-------------------------------------|----------|-------------------|----------------|
| Fully Populated | 256 | 0% | (0,0) | -13.17 | 41.45 | - |
| | | | (8,0) | -13.17 | 40.45 | 1.00 |
| | | | (8,90) | -13.17 | 40.45 | 1.00 |
| Square Tiles | 192 | 25% | (0,0) | -15.82 | 40.90 | - |
| | | | (8,0) | -14.76 | 38.86 | 2.04 |
| | | | (8,90) | -15.47 | 38.86 | 2.04 |
| Square Tiles | 160 | 37% | (0,0) | -14.79 | 41.02 | - |
| | | | (8,0) | -14.37 | 38.49 | 2.53 |
| | | | (8,90) | -14.13 | 38.49 | 2.53 |
| Domino Tiles | 128 | 50% | (0,0) | -13.17 | 41.45 | - |
| | | | (8,0) | -12.02 | 38.40 | 3.05 |
| | | | (8,90) | -11.83 | 37.70 | 3.75 |
| Square Tiles | 124 | 51% | (0,0) | -19.58 | 40.53 | - |
| | | | (8,0) | -13.77 | 36.81 | 3.72 |
| | | | (8,90) | -13.78 | 36.81 | 3.72 |
| Square Tiles | 112 | 56% | (0,0) | -16.85 | 40.53 | - |
| | | | (8,0) | -12.47 | 36.31 | 4.22 |
| | | | (8,90) | -12.84 | 36.31 | 4.22 |
| Multi-Shape #1 Tiles | 112 | 56% | (0,0) | -11.88 | 40.98 | - |
| | | | (8,0) | -10.00 | 35.62 | 5.36 |
| | | | (8,90) | -3.82 | 35.57 | 5.42 |
| Square Tiles | 100 | 61% | (0,0) | -18.89 | 40.56 | - |
| | | | (8,0) | -10.70 | 35.77 | 4.79 |
| | | | (8,90) | -10.70 | 35.77 | 4.79 |
| Multi-Shape #1 Tiles | 100 | 61% | (0,0) | -13.17 | 41.04 | - |
| | | | (8,0) | -10.26 | 33.99 | 7.05 |
| | | | (8,90) | -3.59 | 35.55 | 5.49 |
| Square Tiles | 88 | 66% | (0,0) | -20.44 | 40.61 | - |
| | | | (8,0) | -8.70 | 35.11 | 5.50 |
| | | | (8,90) | -8.26 | 35.12 | 5.49 |
| Multi-Shape #1 Tiles | 88 | 66% | (0,0) | -12.55 | 41.11 | - |
| | | | (8,0) | -9.19 | 33.22 | 7.89 |
| | | | (8,90) | -2.97 | 34.44 | 6.68 |
| Multi-Shape #1 Tiles | 80 | 69% | (0,0) | -12.82 | 41.43 | - |
| | | | (8,0) | -7.31 | 34.89 | 6.55 |
| | | | (8,90) | -7.27 | 34.89 | 6.55 |
| Multi-Shape #2 Tiles | 80 | 69% | (0,0) | -14.56 | 41.02 | - |
| | | | (8,0) | -6.74 | 33.06 | 7.96 |
| | | | (8,90) | -5.52 | 33.02 | 8.00 |
| Square Tiles | 76 | 70% | (0,0) | -12.94 | 40.16 | - |
| | | | (8,0) | -6.97 | 33.26 | 6.90 |
| | | | (8,90) | 0.00 | 33.24 | 6.92 |
| L-Shape Tiles | 64 | 75% | (0,0) | -13.17 | 41.45 | - |
| | | | (8,0) | -6.10 | 31.08 | 10.37 |
| | | | (8,90) | -5.14 | 31.05 | 10.40 |

Table 3.3.2. Array pattern features – Directivity, SLL, and scan-loss, when Isophoric amplifiers are used.

| Architecture | Number of Control Points | Control Points Reduction | Scan Angle (θ, ϕ) [deg] | SLL [dB] | Directivity [dBi] | Scan-Loss [dB] |
|----------------------|--------------------------|--------------------------|-------------------------------------|----------|-------------------|----------------|
| Square Tiles | 112 | 56% | (0,0) | -13.00 | 40.50 | - |
| | | | (8,0) | -13.00 | 36.21 | 4.29 |
| | | | (8,90) | -13.00 | 36.17 | 4.33 |
| Multi-Shape #1 Tiles | 112 | 56% | (0,0) | -13.33 | 40.83 | - |
| | | | (8,0) | -13.00 | 35.95 | 4.88 |
| | | | (8,90) | -13.00 | 35.52 | 5.31 |
| Square Tiles | 100 | 61% | (0,0) | -13.00 | 40.49 | - |
| | | | (8,0) | -13.00 | 35.65 | 4.84 |
| | | | (8,90) | -13.00 | 35.69 | 4.80 |
| Multi-Shape #1 Tiles | 100 | 61% | (0,0) | -13.35 | 41.00 | - |
| | | | (8,0) | -13.00 | 35.28 | 5.72 |
| | | | (8,90) | -13.00 | 35.22 | 5.78 |
| Square Tiles | 88 | 66% | (0,0) | -13.00 | 40.83 | - |
| | | | (8,0) | -13.00 | 34.95 | 5.88 |
| | | | (8,90) | -13.00 | 34.98 | 5.85 |
| Multi-Shape #1 Tiles | 88 | 66% | (0,0) | -13.00 | 41.15 | - |
| | | | (8,0) | -13.00 | 34.65 | 6.50 |
| | | | (8,90) | -13.00 | 34.21 | 6.94 |
| Multi-Shape #1 Tiles | 80 | 69% | (0,0) | -13.00 | 41.34 | - |
| | | | (8,0) | -12.00 | 35.44 | 5.90 |
| | | | (8,90) | -13.00 | 35.25 | 6.09 |
| Multi-Shape #2 Tiles | 80 | 69% | (0,0) | -13.00 | 40.77 | - |
| | | | (8,0) | -13.00 | 34.19 | 6.58 |
| | | | (8,90) | -12.00 | 34.11 | 6.66 |
| Square Tiles | 76 | 70% | (0,0) | -13.00 | 40.91 | - |
| | | | (8,0) | -12.00 | 34.25 | 6.66 |
| | | | (8,90) | -13.00 | 34.27 | 6.64 |
| L-Shape Tiles | 64 | 75% | (0,0) | -13.00 | 41.44 | - |
| | | | (8,0) | -12.00 | 33.61 | 7.83 |
| | | | (8,90) | -12.00 | 32.82 | 8.62 |

Table 3.3.3. Array pattern features – Directivity, SLL, and scan-loss, when considering CP-optimized amplitude and phase excitation coefficients.

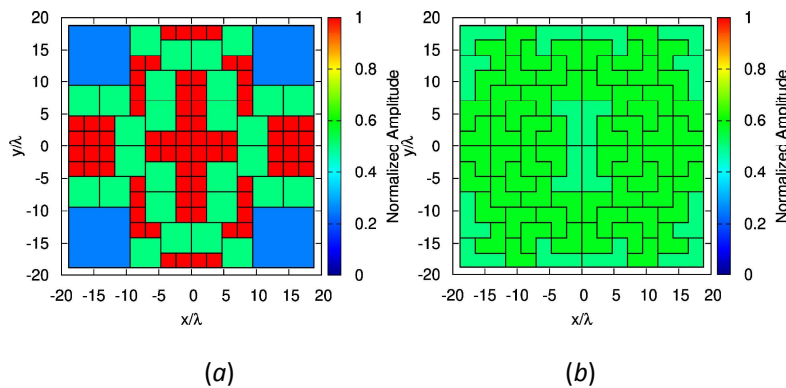


Figure 3.3.2. [TX Band, Isophoric] - Arrangement of the tiles along with the sub-array amplitude for (a) Solution #1 (i.e., Square Shapes – Q = 112) and (b) Solution #2 (i.e., Multi-Shapes #2 – Q=80).

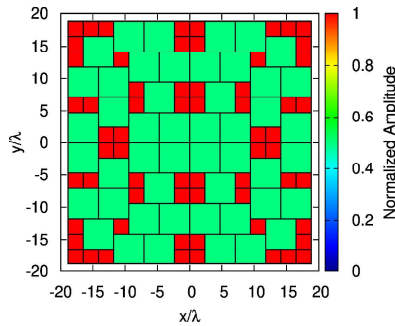


Figure 3.3.3. [Square Tiles, Q=112, TX Band, Isophoric] - Arrangement of the tiles along with the color level representation of the sub-array amplitude of the optimized sub-array configuration.

A better trade-off solution between the number of control points and the Scan-Loss (Fig. 3.3.3) that allow to lower the scan loss to 4.0 [dB] has been finally selected for the partial prototype implementation. The expected performances are analyzed in detail in Deliverable Report D1.7.

3.4. PASSIVE BEAM FORMING NETWORK DESIGN, PROTOTYPE IMPLEMENTATION, AND MEASUREMENTS

A simplified passive beam-forming network (PBFN) is achieved by the design of monolithic components to significantly enhance the simplicity and manufacturability of the entire system. In order to streamline this manufacturing process, hexagonal-shaped waveguide has been employed to enable vertical 3D printing for the realization of these monolithic components. Very solid results have been obtained at all geometry types, with a reflection coefficient around -20 dB and X-PD types above 18 dB over the whole TX-Ka band. These results certify the proposed solution, being the first fully monolithic tiles designed in the existing literature. The design of the PBFN has been documented in Deliverable D1.6, reporting the preliminary RF design of the PBFN for the selected AESA solutions tiles, and in Deliverable D1.7, reporting the detailed design of the tile feed network including the feed chain components, the PBFN, and the complete tile for three geometries, namely, the 1x1 [Fig. 3.4.1(a)], the 2x2 [Fig. 3.4.1(b)], and the 4x4 tile [Fig. 3.4.1(c)] shapes.

INSA-IETR with the collaboration of SWISSto12 has mechanically designed and fabricated one quarter of the MOSAIC antenna (an 8x8 array with 64 elements). The fabrication route is SWISSto12's 3D printing for RF space applications. The MOSAIC antenna is formed by single elements and 2x2-tiles that are designed for vertical 3D printing. The picture of the fabricated partial prototype is reported in Fig. 3.4.2.

The prototype has been evaluated in the IETR anechoic chamber. The results are generally very satisfactory, showing a good matching between the expected and measured beam shapes for both single elements and tiles (Fig. 3.4.3). The testing campaign covered several radiating elements, demonstrating good repeatability among them. Peak directivity and XPD values align well with full-wave simulation predictions. The measurements results are detailed in **Deliverable D1.12**.

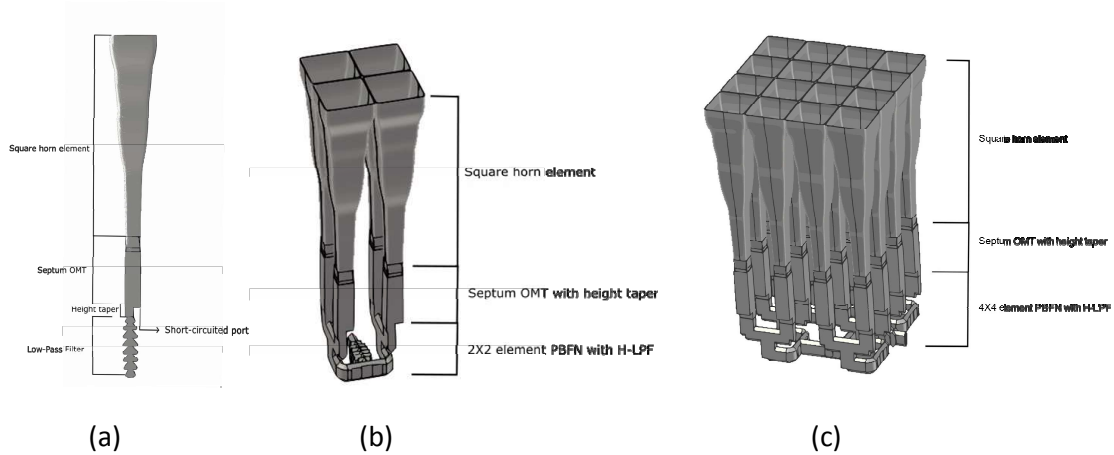


Figure 3.4.1. Schematic of the tiles feed chain.

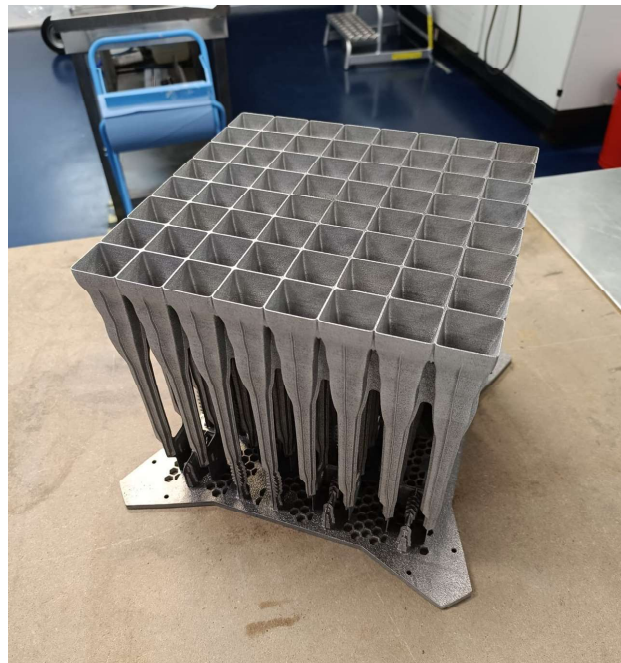


Figure 3.4.2. Prototype fabricated by SWISSto12.

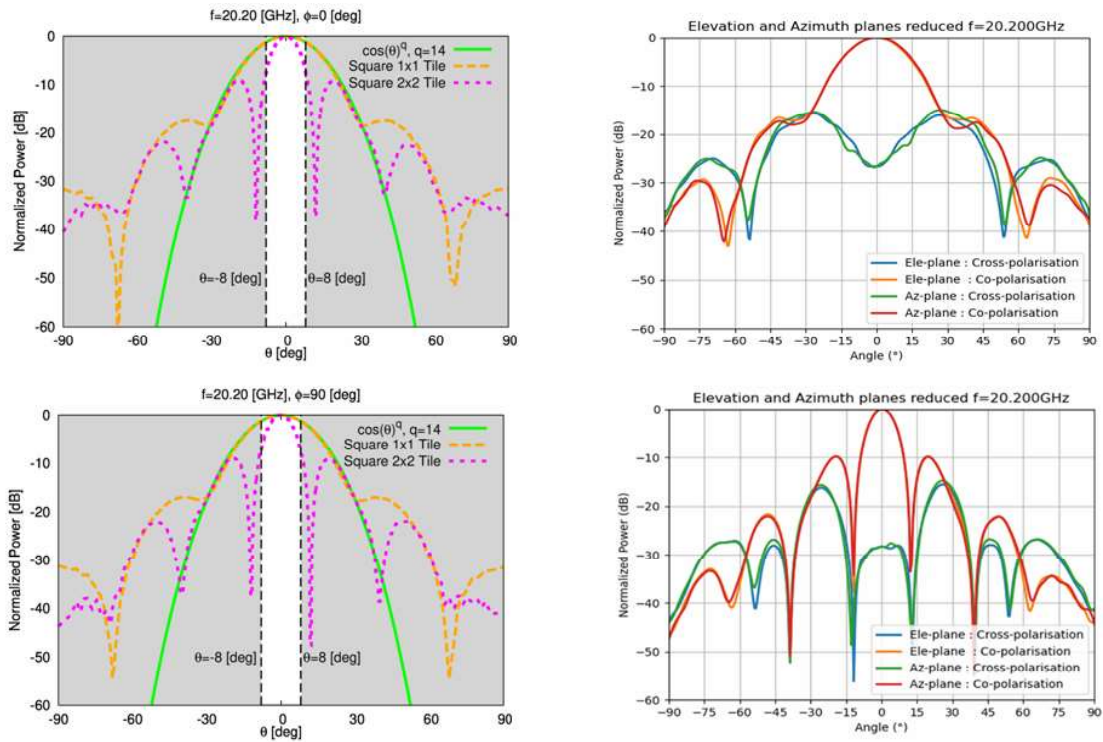


Figure 3.4.3. Single element (i.e., 1x1 tile) and 2x2 square tiles radiation patterns simulated using a full-wave simulator (left column) and measuring the partial prototype (right column).

4. CONCLUSIONS

In conclusion, the MOSAIC project successfully advanced the design and commercial maturity of AESA technology for GEO satellites by building on the ESA invention for large sparse phased arrays. The proposed solution achieved significant innovations, including a 56% reduction in control points through an irregular sub-array architecture, resulting in lower BFN complexity and reduced antenna power consumption. The optimized tile layout minimizes the quantization lobes level and scan-loss while enabling amplifiers to operate in saturation mode. Additionally, the design addressed manufacturing challenges, ensuring simplicity and compatibility with additive manufacturing for RF space applications. Despite performance limitations in the RX frequency band, such as higher SLL and scan-loss, CP optimization demonstrated the potential for improvement.

The outcomes confirm acceptable performance for the project's scope, with opportunities for further enhancement, including reduced scan loss without additional control points and further control point reduction without sacrificing scan loss. Future developments could explore a TX Array-fed Reflector (AFR) with a reduced field-of-view (± 6 degrees) and leverage the L-shape tile configuration to achieve up to a 75% reduction in control points, offering a substantial advancement in sparse array antenna technology.

5. REFERENCES

- [1] C. Mangenot, G. Toso, and C. T. Herrero, "Array antenna with controlled radiation pattern envelope manufacture method," European Patent EP2697865A1, Feb. 19, 2014.
- [2] N. Anselmi, P. Rocca, M. Salucci, and A. Massa, "Irregular phased array tiling by means of analytic schemata-driven optimization" *IEEE Trans. Antennas Propag.*, vol. 65, no. 9, pp. 4495-4510, Sep. 2017.
- [3] P. Rocca, N. Anselmi, A. Polo, and A. Massa, "An irregular two-sizes square tiling method for the design of isophoric phased arrays," *IEEE Trans. Antennas Propag.*, vol. 68, no. 6, pp. 4437-4449, Jun. 2020.
- [4] IETR, "Deliverable Report D1.6 – Project MOSAIC", pp. 1-38, Jul. 4, 2023.